Dynamic response of local pulmonary blood flow to alveolar gas tensions: analysis

BRYDON J. B. GRANT AND ALAN M. SCHNEIDER
Departments of Medicine and Applied Mechanics and Engineering Sciences, University of California San Diego, La Jolla, California 92093; and Department of Internal Medicine, University of Michigan Medical School, Ann Arbor, Michigan 48109

GRANT, BRYDON J. B., AND ALAN M. SCHNEIDER. *Dynamic response of local pulmonary blood flow to alveolar gas tensions: analysis.* J. Appl. Physiol.: Respirat. Environ. Exercise Physiol. 54(2): 445–452, 1983.—It has been reported that left lower lobe pulmonary blood flow ($\dot{Q}$) and alveolar CO_2 decrease then oscillate in a progressively damped manner when the lobar inspirate is changed from pure O_2 to N_2. This damped oscillatory response of lobar $\dot{Q}$ is abolished by maintaining lobar CO_2 constant. We set out to develop the simplest mathematical model that can simulate these experimental results by using techniques derived from control theory. Different models were tested. The simplest model that predicts the experimental data incorporates an exponential decrease of lobar $\dot{Q}$ to local alveolar hypoxia (time constant 3 min) and a damped oscillatory response of lobar $\dot{Q}$ to local alveolar hypocapnia. The response to hypocapnia has two components: a vasodilator effect possibly related to intracellular $[H^+]$ and a vasoconstrictor effect possibly related to changes of molar CO_2. Both these components (time constants of 4.8 min) interact with each other by cross-coupled elements (time constants of 4.8 min). This model can be used to forecast results so that its validity can be tested by experiment.

hypoxic pulmonary vasoconstriction; control theory; oscillations; pulmonary vascular response to carbon dioxide; cycles

HYPOXIC PULMONARY VASOCONSTRICTION is capable of redistributing pulmonary blood flow ($\dot{Q}$) and improving pulmonary gas exchange in the presence of ventilation-perfusion inequality (7–11). Previous analysis of the effects of hypoxic pulmonary vasoconstriction on pulmonary gas exchange have been confined to the steady state. Experiments designed to examine the time course of the hypoxic pulmonary vascular response suggest that it may not be sustained (3, 17, 18, 21), particularly in the presence of alveolar hypocapnia (3, 17). We were intrigued by the results of Benumof et al. (3) because they found that when the lobar inspirate of an anesthetized paralyzed dog is changed from pure O_2 to pure N_2, both lobar $\dot{Q}$ and end-tidal CO_2 (PET_{CO_2}) decreased then oscillated in a progressively damped manner. If lobar alveolar CO_2 was held constant by adding CO_2 to the lobar inspirate during hypoxia, a sustained decrease of lobar $\dot{Q}$ occurred in response to hypoxia within 10 min and no cyclic changes were observed. We were impressed by the long periodicity of these cycles that averaged 40 min, since the vascular responses to both alveolar O_2 and CO_2 appear to be rapid. Although the time course of the pulmonary vascular response to CO_2 has not been studied systematically, data from both Viles and Shephard (25, 26) and Barer et al. (1, 2) appear to show maximal responses to CO_2 within 10 min. Therefore we were unclear as to the mechanisms responsible for the observed damped oscillatory response of lobar $\dot{Q}$ to hypoxia. Any explanation of the physiological basis of hypoxic pulmonary vasoconstriction must take into account the time course of the hypoxic vascular response. Therefore we set out to develop the simplest mathematical model that is capable of explaining the experimental results and has realistic parameters. Such a model could then be used to design experiments to test its validity.

This report describes the development of a nonlinear mathematical model that predicts the experimental data of Benumof et al. (3). We found that it was necessary to explore several variations of basic design of the system to achieve our objective. The salient aspects of the system and its variations are contained in the main text. The mathematical details are provided in the APPENDIX.

METHODS

In this section, we proceed in the following manner. First we present the basic features of the mathematical model. Second we describe the variations of the model that are used to determine whether certain postulates of the relation between components of the pulmonary vascular response to O_2 and CO_2 explain the experimental observations. Third we provide the key features of the mathematical approach to this study.

Basic Features of the System

The experimental preparation used by Benumof et al. (3) enabled the left lower lobe of the anesthetized paralyzed dog to be ventilated with either pure O_2 or hypoxic gas mixtures independently of the rest of the lungs. We assumed that there is no ventilation-perfusion inequality or diffusion defect within the lobe; atelectasis was prevented in his open-chest preparation by the use of positive end-expiratory pressure. We considered the lobar alveolar ventilation to be constant, since the ventilator settings were not altered during the experiment. The rest of the lungs were ventilated with pure O_2. Therefore we assumed that there were no significant changes of sys-

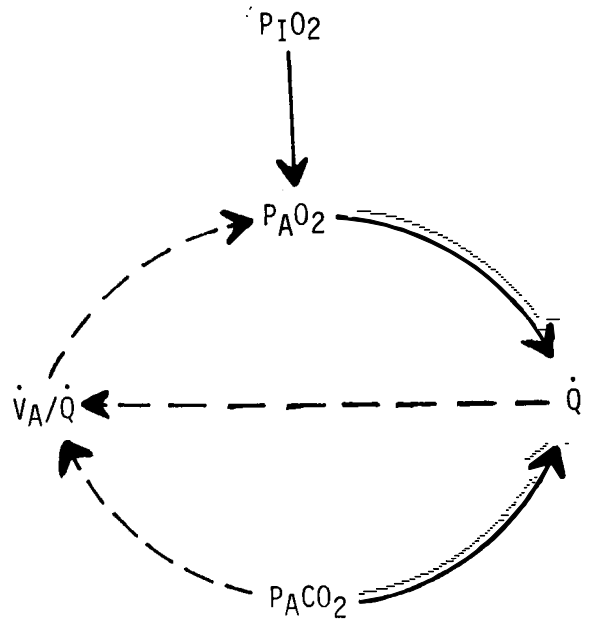

FIG. 1. *Symbol-arrow* diagram of basic design of model. *Arrows* represent working relationships between variables. Primary change of 1 variable leads to secondary change of another variable. *Solid arrows*, direct relations; *interrupted arrows*, indirect relations. If lobar inspired O_2 tension ($P_{I_{O_2}}$) is changed from pure O_2 to pure N_2, lobar alveolar O_2 tension ($P_{A_{O_2}}$) falls, which decreases lobar pulmonary blood flow ($\dot{Q}$) due to hypoxic pulmonary vasoconstriction. Decreased $\dot{Q}$ will increase lobar ventilation-perfusion ratio ($\dot{V}_A/\dot{Q}$). Increased $\dot{V}_A/\dot{Q}$ will decrease both $P_{A_{O_2}}$ and $P_{A_{CO_2}}$ under conditions of N_2 breathing when both inspired O_2 and CO_2 tensions are less than mixed venous blood gas O_2 and CO_2 tensions. Decrease of $P_{A_{CO_2}}$ tends to increase $\dot{Q}$.

temic blood gas composition and cardiac input. With these assumptions, it is necessary only to consider gas exchange in the left lower lobe, since the changes of lobar alveolar gas tensions can occur only from changes of the lobar inspired gas composition or lobar $\dot{Q}$. In addition to these passive mechanisms the model incorporates the active effects of lobar alveolar O_2 and CO_2 tensions ($P_{A_{O_2}}$ and $P_{A_{CO_2}}$, respectively) on $\dot{Q}$. The relations between the active and passive mechanisms are shown in Fig. 1 in the form of a symbol-arrow diagram. A change of the lobar inspirate from pure O_2 to N_2 causes changes in the lobar alveolar gas tensions and $\dot{Q}$ that do not occur instantaneously. By determining the anticipated change of these variables under steady-state conditions and the time delays in the system, differential equations can be obtained that can be used to calculate the actual values of each variable at any instant of time.

Passive mechanisms. Under steady-state conditions the lobar alveolar gas tensions depend on the lobar inspired gas composition, the mixed venous blood gas composition, and the lobar ventilation-perfusion ratio ($\dot{V}_A/\dot{Q}$). If these values are known, the lobar alveolar gas tensions can be calculated from computer subroutines described in detail by West and Wagner (27). N_2 exchange is taken into account. The lobar inspired gas composition is initially 100% O_2. Mixed venous blood gas composition is held constant with values for O_2 tension ($P\bar{v}_{O_2}$) of 40 Torr and CO_2 tension ($P\bar{v}_{CO_2}$) of 46 Torr. Blood gas contents are calculated with a hemoglobin concentration of 14.8 g/100 ml, a hematocrit of 0.45, body temperature of 37°C, and N_2 solubility in blood of 0.0017 vol%. The initial $\dot{V}_A/\dot{Q}$ ratio is set at unity so that the initial $P_{A_{CO_2}}$ is 40 Torr. Since we are concerned only with changes of lobar $\dot{Q}$ with time, lobar $\dot{Q}$ is arbitrarily set at unity under initial conditions to simplify the calculations. Since lobar $\dot{V}_A$ is held constant, changes of lobar $\dot{V}_A/\dot{Q}$ are due to changes of lobar $\dot{Q}$. Although the change of $\dot{V}_A/\dot{Q}$ that occurs with an alteration of $\dot{Q}$ is instantaneous, the changes of $P_{A_{O_2}}$ and $P_{A_{CO_2}}$ are not. The rates of change of the alveolar gas tensions depend on the rate at which O_2 and CO_2 are transferred from the pulmonary capillary blood into the alveoli and the rate which lobar $\dot{V}_A$ removes O_2 and CO_2 from the alveoli and lobar alveolar volume.

For both O_2 and CO_2 the rate of gas transfer from the blood phase is calculated from the lobar $\dot{Q}$ and the blood gas content difference between mixed venous blood and arterialized pulmonary venous blood from the lobe. The blood gas tensions of the arterialized blood ($P_{lpv_{O_2}}$ and $P_{lpv_{CO_2}}$) are assumed to be equal to the alveolar gas tensions. The blood gas contents are calculated from computer subroutines developed by Kelman (13–15), but the O_2 dissociation curve is modified for dog blood (6).

The rate at which O_2 and CO_2 are removed from the alveoli is calculated from the product of lobar expired alveolar ventilation ($\dot{V}_A$) and alveolar gas fraction less the product of lobar inspired alveolar ventilation ($\dot{V}_{AI}$) and inspired gas fraction. The expired $\dot{V}_A$ differs slightly from $\dot{V}_{AI}$ because total gas flux is not zero.

To calculate the rates of change of the alveolar gas tensions, an estimate of lobar alveolar volume is required, not in absolute terms, but relative to $\dot{V}_A$. The ratio of lobar alveolar volume to $\dot{V}_A$ (τ_A) was initially assumed to be 0.5 min. This time constant is an important parameter. Therefore we measured this time constant experimentally in a preparation similar to that described by Benumof et al. (3) and found values close to 0.5 min (see APPENDIX A). We found that the change of inspired gas composition as measured in the lobar bronchus was not instantaneous because of delays caused by the Harvard pump and associated tubing. The time constant for a change of lobar inspired gas composition (τ_I) was approximately 0.66 min.

Active mechanisms. To incorporate the effects of $P_{A_{O_2}}$ and $P_{A_{CO_2}}$ on lobar $\dot{Q}$, it is necessary to define their steady-state relations. The steady-state relation between $P_{A_{O_2}}$ and $\dot{Q}$ is shown in Fig. 2*A*. Linear equations are

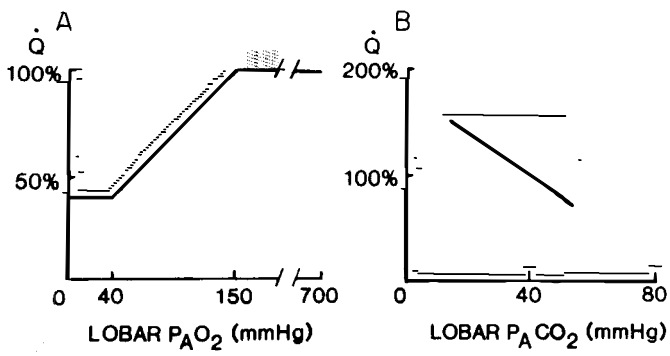

FIG. 2. Graphic representation of steady-state response relations between lobar $\dot{Q}$ and lobar $P_{A_{O_2}}$ (*A*) and between lobar $\dot{Q}$ and $P_{A_{CO_2}}$ (*B*). Abbreviations as in Fig. 1.

used to approximate the sigmoid relation described by Benumof and Wahrenbrock (4). It may not represent the true steady-state relation, since Sylvester and his colleagues (18, 21) have demonstrated hypoxic pulmonary vasodilation when $P_{A_{O_2}}$ is less than 25 Torr. However, variations of the response curve are considered later.

The steady-state relation between $P_{A_{CO_2}}$ and $\dot{Q}$ is shown in Fig. 2*B*. An inverse linear relation is used, in keeping with experimental data of Barer et al. (1), but increased to provide a 2% increase of $\dot{Q}$ per unit fall of $P_{A_{CO_2}}$ so that results are compatible with the data of Benumof et al. (3). There is evidence that the pulmonary vascular response to $P_{A_{CO_2}}$ comprises vasodilator and vasoconstrictor components (25, 26). Nevertheless the net results of these components must cause a net vasodilator response to hypocapnia in the model, since Benumof et al. (3) found that the decrease of lobar blood flow with hypoxia was greater under eucapnic than hypocapnic conditions.

None of these pulmonary vascular responses to changes of $P_{A_{O_2}}$ or $P_{A_{CO_2}}$ are instantaneous. We assume initially that both the hypoxic and hypocapnic vascular responses are first-order reactions and can be described by a single time constant for each response. The time constant for the hypoxic vascular response is adjusted so that the model predicts the experimentally observed changes of lobar $\dot{Q}$ due to hypoxia when $P_{A_{CO_2}}$ was held constant (3). The time constant for the hypocapnic vascular response is unknown, but it was varied over a wide range (up to 50 min).

Variations of the System

To obtain a model of predictive value, it is necessary to explore several variations of this model. The modifications we made are summarized in Figs. 3 and 4. For reference the active components of the basic design (Fig. 1) are shown in more detail in Fig. 3*A*. There is a vascular response to both $P_{A_{O_2}}$ and $P_{A_{CO_2}}$, which act independently of each other with exponential decays toward des-

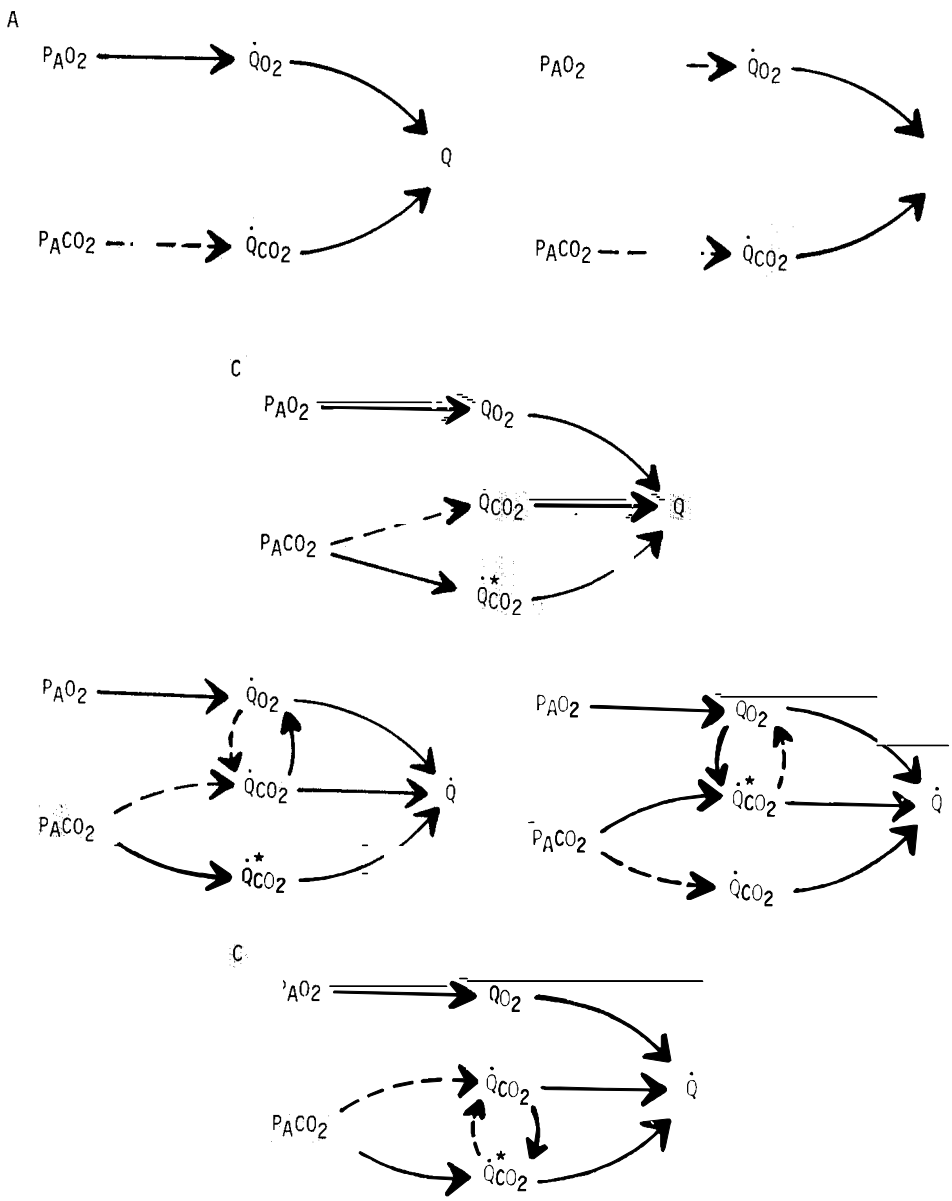

FIG. 3. *Symbol-arrow* diagrams that show some modifications of basic model. *A*, hypoxic pulmonary vasoconstriction and hypocapnic vasodilation act independently of each other. Changes of $\dot{Q}$ due to $P_{A_{O_2}}$ and $P_{A_{CO_2}}$ are represented by $\dot{Q}_{O_2}$ and $\dot{Q}_{CO_2}$, respectively. *B*, independent effects of hypoxic pulmonary vasodilation and hypocapnic vasodilation. *C*, hypoxic pulmonary vasoconstriction, hypocapnic vasodilation, and hypocapnic vasoconstriction, all with separate effects of lobar $\dot{Q}$. Changes of $\dot{Q}$ due to hypocapnic vasodilation and hypocapnic vasoconstriction are represented by $\dot{Q}_{CO_2}$ and $\dot{Q}^*_{CO_2}$, respectively. Abbreviations as in Fig. 1.

FIG. 4. *Symbol-arrow* diagrams of interactions between hypoxic vasoconstriction, hypocapnic vasodilation, and hypocapnic vasoconstriction. *A*, interaction by cross-coupled elements between hypoxic pulmonary vasoconstriction and hypocapnic vasodilation. *B*, interaction between hypoxic pulmonary vasoconstriction and hypocapnic vasoconstriction. *C*, interaction between hypocapnic vasodilation and hypocapnic vasoconstriction that is independent of hypoxic pulmonary vasoconstriction. Abbreviations as in Figs. 1 and 4.

ignated steady-state values. The rates of these changes are varied by adjusting the time constants for each response. The shape of the hypoxic pulmonary vascular response curve is also varied. Figure 3*B* uses a hypoxic pulmonary vasodilator response that may occur if there is a severe degree of hypoxia. Both these models suppose that there is a hypocapnic vasodilator response. Some investigators have suggested that the pulmonary vascular response to CO_2 is more complex.

Viles and Shephard (25, 26) suggested that the pulmonary vascular response to CO_2 has two components: a hypocapnic vasodilator response due to decrease of $[H^+]$ and a vasoconstrictor response due to decreases of molar CO_2 (Fig. 3*C*). They also suggested a relationship between changes of intracellular $[H^+]$ and hypoxic pulmonary vasoconstriction. This idea is extended to consider a hypoxic vasoconstrictor effect, a hypocapnic vasodilator effect, and a hypocapnic vasoconstrictor effect with an interaction between two of these three mechanisms that affects both dynamic and steady-state responses. An interaction is introduced into the system by the use of cross-coupled terms. For example, interaction between the hypoxic vasoconstrictor response and the hypocapnic vasodilator response occurs because the hypoxic vasoconstrictor response potentiates hypocapnic vasodilation and hypocapnic vasodilator response attenuates hypoxic vasoconstriction (Fig. 4*A*). Each of these cross-coupled elements is assigned a gain and is considered a first-order reaction. Similarly interactions can be introduced between hypoxic vasoconstriction and hypocapnic vasoconstriction (Fig. 4*C*). In all three models represented in Fig. 4 the sign of the cross-coupled elements (attenuation or potentiation) was varied as well as their gain and time constant.

Computer Formulation of the Model

The computer program is used to produce a plot of lobar $\dot{Q}$ vs. time when the composition of the lobar inspirate is changed. First the initial conditions are set so that lobar $P_{A_{CO_2}}$ is 40 Torr with normal mixed venous blood gas composition when the lobe is ventilated with O_2. The differentiation equations (see APPENDIX B) that describe the rate of change of inspired gas composition and the rates of change of $P_{A_{O_2}}$ and $P_{A_{CO_2}}$ with respect to the time are integrated numerically with a fourth-order Runge-Kutta-Gill method (19). The procedure is used to determine the values of lobar $\dot{Q}$, $P_{A_{O_2}}$, and $P_{A_{CO_2}}$ at 1-min intervals. These plots are then compared with Benumof's experimental data. This approach is an extremely time-consuming method to explore the dynamic characteristics of the system because of the large number of time constants and gains that need to be tested. We found that a more convenient approach is to use a linear approximation of the nonlinear system.

Linear approximation. The dynamic response of each system and its variations that were tested are determined by writing the differential equations in algebraic form. The O_2 and CO_2 dissociation curves and pulmonary vascular response curves to CO_2 are linearized. Any nonlinearities that arise in the course of linearizing the differential equations are ignored. The simultaneous first-order differential equations are solved by matrix algebra to obtain the characteristic equation of the system (see APPENDIX C). The roots of this polynomial expression are used to predict the dynamic response (Fig. 5). The roots of the polynomial expression are determined by a numerical method in a separate computer program (subroutine ZPOLY, International Mathematical and Statistical Libraries, Houston, TX). The system parameters are varied until the desired pair of complex roots is obtained that would indicate damped oscillatory response of lobar $\dot{Q}$. Since this approach is an approximation and only tests the dynamic response of the system, it is necessary to check that these parameters give both the desired dynamic and steady-state responses of lobar $\dot{Q}$ to changes in the composition of the lobar inspirate. Nevertheless the linear approximation proved to be a close approximation of the nonlinear dynamic response.

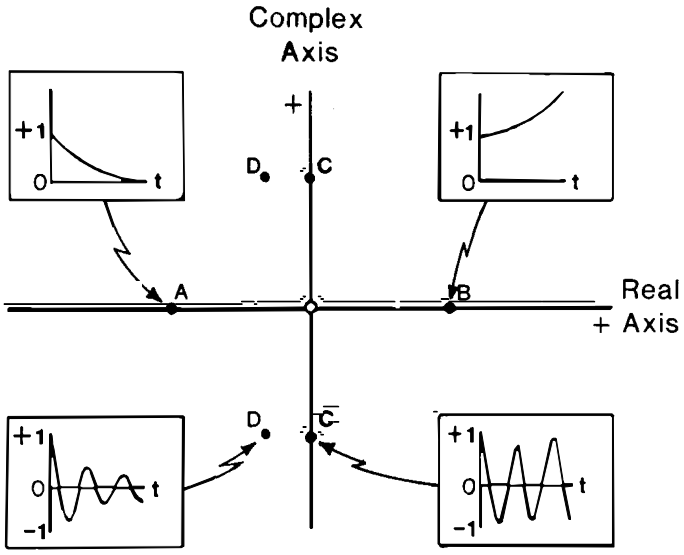

FIG. 5. Root locus plot to demonstrate that dynamic response can be predicted from eigenvalues roots of characteristic equation of linearized model. *Abscissa*, real axis; *ordinate*, complex or imaginary axis. *A*, negative real root that will produce exponential decrease as time increases. *B*, positive real root signifying response that increases without bound. *C*, pair of complex roots with no real component that produces sustained oscillations. *D*, pair of complex roots with no real component that produces sustained oscillations. *D*, pair of complex roots with negative real component that produces progressively damped oscillatory response as time increases.

RESULTS

Pulmonary Vascular Response to O_2 and CO_2 Acting Independently

Our first attempts to simulate Benumof's experimental data did not incorporate any interaction between the effects of hypoxia and hypocapnia on the pulmonary vasculature. Three variations were tested. *1*) Hypoxia caused lobar $\dot{Q}$ to decrease monotonically with increasing degrees of hypoxia with hypocapnia opposing hypoxic vasoconstriction (Fig. 3*A*). This model is similar to the mechanism proposed by Benumof et al. (3). *2*) Hypoxic vasodilation at extreme degrees of hypoxia was incorporated into the model (Fig. 3*B*) in keeping with the experimental data of Sylvester et al. (21). Both these

models suffered the same problem: a damped oscillatory response to ventilation of the lobe with pure N_2 did not occur unless the ratio of lobar alveolar volume to $\dot{V}_A$ (time constant τ_A) is greater than 20 min. Our own experimental data indicates that this value of τ_A is unrealistic, since our measurements indicate that it is approximately 0.5 min. Therefore these two models were rejected. *3)* We separated the pulmonary vascular response to CO_2 into two components (Fig. 3*C*). Since the time courses of the vascular response to molar CO_2 and $[H^+]$ are unknown, wide variations of the time constants of these effects were used (0–40 min). Damped oscillatory responses of lobar $\dot{Q}$ could be obtained in response to N_2 breathing, but the model was unstable. For example, if a hypoxic vascular response was produced under isocapnic conditions by using 5% CO_2 in N_2 as the inspired gas, negative values of lobar $\dot{Q}$ occurred when CO_2 is removed from the lobar inspirate. In view of these failures to simulate the experimental data, we supposed that there must be an interaction between at least two of the three components of the pulmonary vascular response to O_2, $[H^+]$, and molar CO_2.

Interactions Between Pulmonary Vascular Responses to O_2 and CO_2

Several investigators (5, 16, 25, 26) have suggested an interaction between the vascular responses to O_2 and CO_2. We tested models with an interaction between hypoxic pulmonary vasoconstriction and hypocapnic vasodilation due to changes of $[H^+]$ (Fig. 4*A*) and between hypoxic pulmonary vasoconstriction and hypocapnic vasoconstriction due to changes of molar CO_2 (Fig. 4*B*). Both models had two major drawbacks: *1)* a damped oscillatory response of lobar $\dot{Q}$ to hypoxia occurs even under isocapnic conditions; and *2)* the correct dynamic and steady-state responses could not be obtained simultaneously. The correct dynamic behavior could be obtained only with an incorrect steady-state response. For example, lobar $\dot{Q}$ during N_2 breathing exceeded its value during O_2 breathing. Alternatively the correct steady-state response could be obtained only with an incorrect dynamic response. For example, lobar $\dot{Q}$ decreased initially if the lobar inspired gas is changed from 5% CO_2 in N_2 to pure N_2. These difficulties lead us to consider the possibility that the vascular responses of O_2 and CO_2 are independent of each other, but there is an interaction between the two components of the CO_2 response (Fig. 4*C*).

Interaction Between Components of Pulmonary Vascular Response to CO_2

The model (Fig. 4*C*) that predicts most successfully the experimental data has an interaction between both components of the vascular response to CO_2. The hypoxic vascular response curve with a time constant of 3 min was used (Fig. 2). The hypocapnic vasodilator response has a gain of $-2\%\ \Delta\dot{Q}/\Delta P_{A_{CO_2}}$ Torr, and the hypocapnic vasoconstrictor response has a gain of $+2\%\ \Delta\dot{Q}/\Delta P_{A_{CO_2}}$. The time constant of both responses is 4.8 min. Interaction is introduced by cross-coupled elements such that

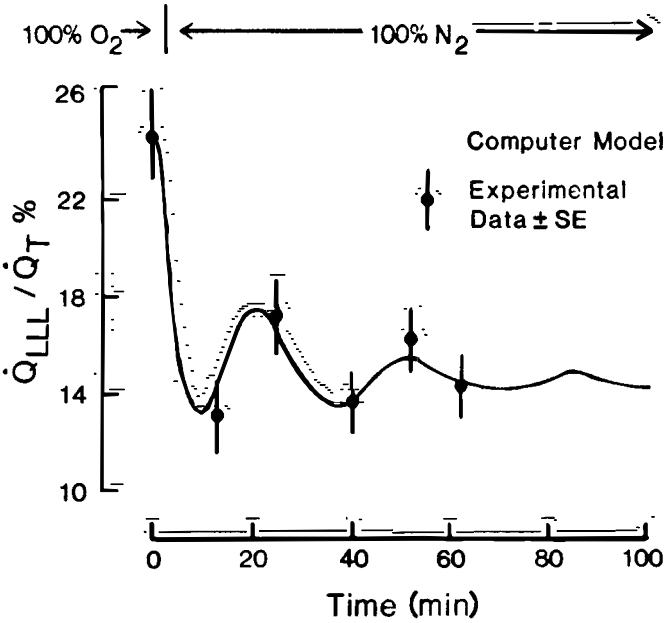

FIG. 6. Comparison of changes of lobar pulmonary blood flow expressed as proportion of total flow ($\dot{Q}_{LLL}/\dot{Q}_T$, %, *ordinate*) that occur with time in minutes (*abscissa*) between experimental data obtained from Fig. 3 of Ref. 3 and computer model. This graph shows that computer model is capable of simulating experimental data when left lower lobe inspirate is changed from pure O_2 to pure N_2.

hypocapnic vasodilation suppresses hypocapnic vasoconstriction (gain of $+1.28\ \Delta\dot{Q}\ddot{c}_{O_2}/\Delta\dot{Q}c_{O_2}$) and hypocapnic vasoconstriction potentiates hypocapnic vasodilation (gain of $-1.28\ \Delta\dot{Q}c_{O_2}/\Delta\dot{Q}\ddot{c}_{O_2}$). Both elements have time constants of 4.8 min. The net steady-state response of lobar $\dot{Q}$ to both components of the CO_2 response is $-1.9\%\ \Delta\dot{Q}/\Delta P_{A_{CO_2}}$ Torr. Figure 6 compares the experimental data points (Fig. 3 of Ref. 3) with the computer simulation when the lobar inspirate is changed from pure O_2 to pure N_2. The values of lobar $\dot{Q}$ from the computer model are rescaled to express these values in terms of the proportion of total $\dot{Q}$ to the left lower lobe ($\dot{Q}_{LLL}/\dot{Q}_T$). Figure 7 compares the experimental data points (Fig. 4 of Ref. 3) with the computer simulation when the lobar inspirate is changed from pure O_2 to N_2 with added CO_2 to maintain $P_{A_{CO_2}}$ constant. By maintaining isocapnia the damped oscillatory response of lobar $\dot{Q}$ to hypoxia no longer occurs. But if CO_2 is withdrawn from the lobar inspirate, oscillatory changes of lobar $\dot{Q}$ occur, just as Benumof et al. (Fig. 5 of Ref. 3) described in two experiments. Both experimental results are simulated with the same model parameters. The computer simulation produced results that are within 1 SE of the experimental data points.

DISCUSSION

Our general approach to finding a model that is capable of predicting the experimental data (3) is to start with a basic model and then increase its complexity until a model of predictive value is obtained. We failed to achieve this objective with earlier versions of the system (Fig. 3). Therefore we believe that there must be an interaction between the mechanisms by which O_2 and

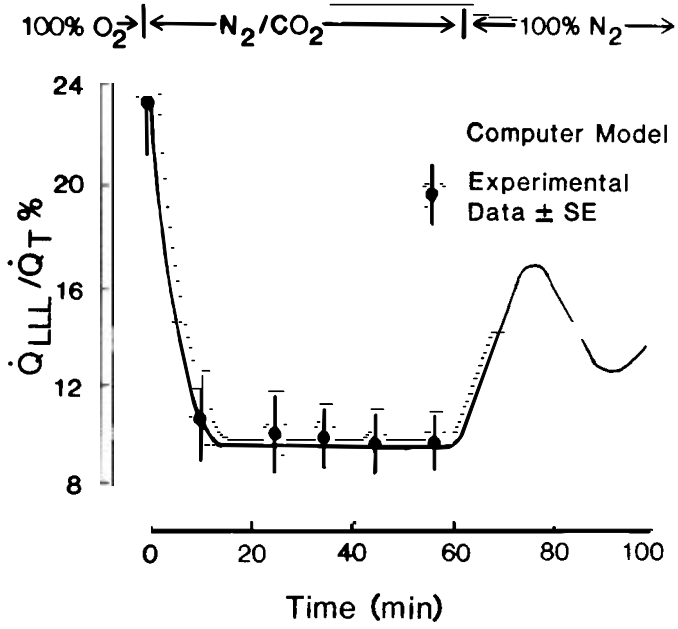

FIG. 7. Comparison of changes of lobar pulmonary blood flow expressed as proportion of total flow ($\dot{Q}_{LLL}/\dot{Q}_T$, %, *ordinate*) that occur with time in minutes (*abscissa*) between experimental data obtained from Fig. 4 of Ref. 3 and computer model. This graph shows that computer model is capable of simulating experimental data when left lower lobe inspirate is changed from pure O_2 to N_2 with added CO_2 to maintain local isocapnia. At 60 min lobe was ventilated with pure N_2 and computer model shows an oscillatory response similar to that observed in 2 experiments (data points not shown) in Fig. 5 of Ref. 3.

CO_2 produce their effects on the pulmonary vasculature. Without such an interaction the experimental data can be simulated only with values of the time constant for the rate of change of alveolar gas tensions (τ_A) we showed to be experimentally unrealistic.

Our approach, to develop the simplest model of predictive value, has limitations. This model may not be the correct model or the only model; indeed earlier versions with some modifications may yet prove to be valid. For example, if the interaction between hypoxic pulmonary vasoconstriction and hypocapnic vasodilation only occurred below a threshold value of $P_{A_{CO_2}}$, then this model would be capable of simulating the experimental data. We supposed that the dynamic response is the result of a system with linear dynamic characteristics because of the sinusoidal nature of the cyclic changes of lobar $\dot{Q}$ and $P_{A_{CO_2}}$ of the damped oscillatory response observed experimentally (3). Oscillatory behavior can occur due to nonlinearities in the system, but in these cases the cyclic changes tend to be asymmetric (12).

The main features of the model that we propose to explain Benumof's experimental data are a monotonic response of lobar $\dot{Q}$ to changes of $P_{A_{O_2}}$ and a damped oscillatory response of lobar $\dot{Q}$ to changes of $P_{A_{CO_2}}$. However, not all studies agreed that there is a monotonic response of lobar $\dot{Q}$ to hypoxia even under isocapnic conditions (18, 21, 22). Indeed in vitro data of Sylvester et al. (21) suggest a transient overshoot of pulmonary vascular tone at severe degrees of hypoxia. Therefore the first-order hypoxic vascular response does not explain all the experimental data concerning the dynamics of hypoxic pulmonary vasoconstriction in different species. The damped oscillatory response of $\dot{Q}$ to $P_{A_{CO_2}}$ in our model is due to interaction between the two components of the effect of CO_2. Interaction between these vasodilator and vasoconstrictor effects of CO_2 has not been demonstrated experimentally. This interaction is produced by the introduction of cross-coupled elements. There is evidence to support the idea that cross-coupled mechanisms exist in biochemical systems. Indeed attempts have been made to link the autooscillations of systemic arterial smooth muscle with oscillations in the glycolytic pathway, although these 1- to 10-min autooscillations should be distinguished from the 40-min oscillations generated by this model (20). Other biochemical pathways may be involved. For example, there may be interactions between the vasoconstrictor effects of H_1 receptors and the vasodilator effects of H_2 receptors (23) by histamine, which appears to be released during hypoxia (24).

Regardless of the limitations of this study, the model that we have developed does provide a useful basis for further experimentation. A detailed understanding of the dynamic response of the pulmonary vasculature to changes of alveolar gas tensions will be required to elucidate the physicochemical basis of this phenomenon.

APPENDIX

A. Measurement of Time Constant

To measure the time constant (τ_A) for the rate of change of alveolar gas tensions, we anesthetized 2 mongrel dogs (20.2 and 28.4 kg) with 25 mg pentobarbital per kg body wt and set up the preparation as described by Benumof et al. (3). In brief a cannula was inserted into the left lower lobe bronchus in an open-chest preparation. The left lower lobe was ventilated independently of the rest of the lungs with a dual Harvard pump on 5 cmH_2O positive end-expiratory pressure. The left lower lobe was ventilated with approximately 10% He in O_2 and the rest of the lungs with pure O_2. Ventilation of the left lower lobe and the rest of the lung were adjusted so that arterial P_{CO_2} was 40 Torr and the respective airway pressure swings were equalized. Dead space was added to the bronchial cannula so that $P_{ET_{CO_2}}$, measured by a Perkin-Elmer mass spectrometer, in the bronchial cannula was equal to the $P_{ET_{CO_2}}$ in the rest of the lungs. The left lower lobe was equilibrated with the He gas mixture as judged by the lack of difference between inspired and expired He fraction measured with the mass spectrometer. Then the lobar inspirate was changed to pure O_2 by changing the lobar inspired gas supply to the Harvard pump. The changes of inspired and end-tidal (alveolar) He gas fraction were measured breath by breath ($F_{I_{He}}$ and $F_{A_{He}}$, respectively). Because of delays caused by the tubing and the ventilator the change of $F_{I_{He}}$ as measured in the bronchial cannula is not instantaneous but a complex function of time. The ventilatory frequency was measured to obtain the total time for each breath (t_B).

Since He is a relatively insoluble gas, elimination of He from body stores is negligible. Therefore only He elimination from the alveolar gas of the left lower lobe needed to be considered. The He washout for each breath was described by the equation

$$d(F_{I_{He}})/dt = [F_{I_{He_{(n+1)}}} - F_{I_{He_{(n)}}}]/t_B$$

$$d(F_{A_{He}})/dt = [F_{I_{He_{(n)}}} - F_{A_{He_{(n)}}}]/\tau_A$$

where subscript n is the breath number. A computer program with a Runge-Kutta-Gill integration procedure predicted $F_{A_{He}}$ for each breath with a given value of τ_A, the initial value of $F_{A_{He}}$, and the measured values of $F_{I_{He}}$ for 9–12 breaths. The calculated values of $F_{A_{He_{(n)}}}$ are then compared with the measured values of $F_{A_{He_{(n)}}}$; τ_A is adjusted to obtain the best estimate by least-squares approximation. The correlation coefficients between measured and predicted values of $F_{A_{He_{(n)}}}$ were always greater than 0.997. The three estimates of τ_A were made: values were 0.45 and 0.54 min in the 20.2-kg dog and 0.35 min in the 28.4-kg dog.

B. Differential Equations for Nonlinear Model

The differential equations given in this section are those used in the variation of the basic model shown in Fig. 3*F*. At any moment in time it is necessary to calculate the steady-state changes of $\dot{Q}$ due to hypoxic pulmonary vasoconstriction [$\dot{Q}o_{2(\infty)}$], hypocapnic vasodilation [$\dot{Q}co_{2(\infty)}$], and hypocapnic vasoconstriction ($\dot{Q}^{*}co_{2(\infty)}$) for the prevailing level of $P_{A_{O_2}}$ and $P_{A_{CO_2}}$ at that moment. Therefore

$$\dot{Q}o_{2(\infty)} = D_1 \cdot [P_{A_{O_{2(t)}}} - P_{A_{O_{2(0)}}}] + c \tag{1}$$

where D_1 and c depend on which of the three linear relations are applicable for the value of $P_{A_{O_{2(t)}}}$, and $[P_{A_{O_{2(t)}}} - P_{A_{O_{2(0)}}}]$ is the change of $P_{A_{O_2}}$ from initial conditions (0) at any moment in time (t).

$$\dot{Q}co_{2(\infty)} = D_2 \cdot [P_{A_{CO_{2(t)}}} - P_{A_{CO_{2(0)}}}] + A_{(t)} \tag{2}$$

where D_2 is the gain of the hypocapnic vasodilator response, $[P_{A_{CO_{2(t)}}} - P_{A_{CO_{2(0)}}}]$ is the change of $P_{A_{CO_2}}$ from initial conditions, and A is the change of $\dot{Q}co_2$ due to potentiation of $\dot{Q}co_2$ by $\dot{Q}^{*}co_2$.

$$\dot{Q}^{*}co_{2(\infty)} = D_3 \cdot [P_{A_{CO_{2(t)}}} - P_{A_{CO_{2(0)}}}] + B_{(t)} \tag{3}$$

where D_3 is the gain of the hypocapnic vasoconstrictor response and B is the change of $\dot{Q}^{*}co_2$ due to attenuation of $\dot{Q}^{*}co_2$ by $\dot{Q}co_2$. The steady-state values of A and B are defined as

$$A_{(\infty)} = K_1 \cdot \dot{Q}^{*}co_{2(t)} \tag{4}$$

$$B_{(\infty)} = K_2 \cdot \dot{Q}co_{2(t)} \tag{5}$$

where K_1 is the gain of the effect of the hypocapnic vasoconstrictor response on hypocapnic vasodilation and K_2 is the gain of the effect of the hypocapnic vasodilator response on hypocapnic vasoconstriction. At any moment in time the value of $\dot{Q}$ [$\dot{Q}_{(t)}$] is the sum of the instantaneous values of $\dot{Q}o_2$, $\dot{Q}co_2$, and $\dot{Q}^{*}co_2$ and the initial value of $\dot{Q}$ [$\dot{Q}_{(0)}$]. Therefore

$$\dot{Q}_{(t)} = \dot{Q}(0) + \dot{Q}o_{2(t)} + \dot{Q}co_{2(t)} + \dot{Q}^{*}co_{2(t)} \tag{6}$$

To calculate the values of $\dot{Q}_{(t)}$ at each time interval, the following simultaneous differential equations were integrated numerically.

$$dP_{I_{O_2}}/dt = [P_{I_{O_{2(\infty)}}} - P_{I_{O_{2(t)}}}]/\tau_1 \tag{7}$$

$$dP_{I_{CO_2}}/dt = [P_{I_{CO_{2(\infty)}}} - P_{I_{CO_{2(t)}}}]/\tau_1 \tag{8}$$

$$dP_{A_{O_2}}/dt = \{[P_{I_{O_{2(t)}}} \cdot \dot{V}_{AI}/\dot{V}_{A(t)} - [P_{A_{O_{2(t)}}}]/0.863 - 10 \cdot (\dot{Q}_{(t)}/\dot{V}_A) \cdot [Clpv_{O_{2(\infty)}} - C\bar{v}_{O_2}]\}/\tau_A \tag{9}$$

$$dP_{A_{CO_2}}/dt = \{[P_{I_{CO_{2(t)}}} \cdot \dot{V}_{AI}/\dot{V}_{A(t)} - P_{A_{CO_2}}]/0.863 - 10 \cdot (\dot{Q}_{(t)}/\dot{V}_A) \cdot [Clpv_{CO_{2(t)}} - C\bar{v}_{CO_2}]\}/\tau_A \tag{10}$$

$$d\dot{Q}o_2/dt = [\dot{Q}o_{2(\infty)} - \dot{Q}o_{2(t)}]/\tau_3 \tag{11}$$

$$d\dot{Q}co_2/dt = [\dot{Q}co_{2(\infty)} + A_{(t)} - \dot{Q}co_{2(t)}]/\tau_4 \tag{12}$$

$$d\dot{Q}^{*}co_2/dt = [\dot{Q}^{*}co_{2(\infty)} + B_{(t)} - \dot{Q}^{*}co_{2(t)}]/\tau_5 \tag{13}$$

$$dA/dt = [K_1 \cdot \dot{Q}^{*}co_{2(t)} - A_{(t)}]/\tau_6 \tag{14}$$

$$dB/dt = [K_2 \cdot \dot{Q}co_{2(t)} - B_{(t)}]/\tau_7 \tag{15}$$

where $P_{I_{O_2}}$ and $P_{I_{CO_2}}$ are inspired O_2 and CO_2 gas tensions, $Clpv_{O_2}$ and $Clpv_{CO_2}$ are lobar pulmonary venous O_2 and CO_2 blood gas contents, respectively, and $C\bar{v}_{O_2}$ and $C\bar{v}_{CO_2}$ are mixed venous O_2 and CO_2 blood gas contents, respectively. The time constants (τ) for each equation are parameters assigned values as described in the main text. $\dot{V}_{AI}$, $C\bar{v}_{O_2}$, and $C\bar{v}_{CO_2}$ are constants, but $\dot{V}_{A(t)}$ does vary slightly from $\dot{V}_{AI}$, depending on the total gas flux between the alveoli and lobar pulmonary capillary blood.

C. Linear Model to Determine Dynamic Characteristics

This system will be used to describe the derivation of the differential equations that are used to determine the dynamic response of $\dot{Q}$ to changes of $P_{A_{O_2}}$ and $P_{A_{CO_2}}$ when the lobar inspirate is changed from O_2 to N_2. Because matrix algebra is used to solve these differential equations, the notation described in the preceding section will be changed to a form consistent with control theory usage. Changes of $P_{A_{O_2}}$, $P_{A_{CO_2}}$, and $P_{I_{O_2}}$ will be denoted by x_1, x_2, and u, respectively. $\dot{Q}o_2$, $\dot{Q}co_2$, $\dot{Q}^{*}co_2$, A, and B will be denoted by x_3, x_4, x_5, x_6, and x_7, respectively. Rates of change of x_n will be denoted by $\dot{x}_n$. The differential *Eqs. 11–15* are already in a linear form. By substituting for $\dot{Q}o_{2(\infty)}$, $\dot{Q}co_{2(\infty)}$, and $\dot{Q}^{*}co_{2(\infty)}$ from *Eqs. 1–3* into *Eqs. 11–13* and by using the revised notation, these differential equations become

$$\dot{x}_3 = (D_1 x_1 - x_3)/\tau_3 \tag{16}$$

$$\dot{x}_4 = (D_2 x_2 + x_6 - x_4)/\tau_4 \tag{17}$$

$$\dot{x}_5 = (D_3 x_2 + x_7 - x_5)/\tau_5 \tag{18}$$

$$\dot{x}_6 = (K_1 x_5 - x_6)/\tau_6 \tag{19}$$

$$\dot{x}_7 = (K_2 x_4 - x_7)/\tau_7 \tag{20}$$

To linearize the first-order differential *Eqs. 9* and *10*, the O_2 and CO_2 dissociation curves are considered to be linear with Ostwald's partition coefficients λ_{O_2} and λ_{CO_2} (3.9 and 4.1, respectively). Differences between $\dot{V}_{AI}$ and $\dot{V}_A$ are ignored, and blood gas tensions in the arterialized blood are set equal to the alveolar gas tensions. Under steady-state conditions *Eq. 9* becomes

$$0 = \{(P_{I_{O_2}} - P_{A_{O_2}}) - \lambda_{O_2} \cdot (P_{A_{O_2}} - P\bar{v}_{O_2}) \cdot [\dot{Q}_{(0)}/\dot{V}_A]\}/\tau_A \tag{21}$$

Under perturbed conditions at any instant

$$\dot{Q} = \dot{Q}_{(0)} + x_3 + x_4 + x_5$$

Therefore under perturbed conditions

$$\dot{x}_1 = \{[P_{I_{O_2}} + u - (P_{A_{O_2}} + x_1)] - \lambda_{O_2} \cdot (P_{A_{O_2}} + x_1 - P\bar{v}_{O_2})\} [\dot{Q}_{(0)} + x_3 + x_4 + x_5]/\dot{V}_A\}/\tau_A \tag{22}$$

By subtracting *Eq. 21* from *22* and ignoring any nonlinear terms, justified on the basis of being second order or higher, we obtain the following expression

$$\dot{x}_1 = -\{[\lambda_{O_2} \cdot \dot{Q}_{(0)}]/(\dot{V}_A \cdot \tau_A) + 1\} x_1 + \{\lambda_{O_2} \cdot [P\bar{v}_{O_2} - P_{A_{O_{2(0)}}}]/(\tau_A \cdot \dot{V}_A)\} \cdot (x_3 + x_4 + x_5) + u/\tau_A \tag{23}$$

A similar expression can be obtained for CO_2

$$\dot{x}_2 = -\{[\lambda_{CO_2} \cdot \dot{Q}_{(0)}]/(\dot{V}_A \cdot \tau_A) + 1\} \cdot x_2 + \{\lambda_{CO_2} \cdot [P\bar{v}_{CO_2} - P_{A_{CO_{2(0)}}}]/(\tau_A \cdot \dot{V}_A)\} \cdot (x_3 + x_4 + x_5) \tag{24}$$

Now we have seven linear first-order differential equations that can be rewritten in the general form, where $a_{i,j}$ are coefficients of x_i where i and j are 1, 2, ..., 7.

$$\dot{x}_i = a_{i,1} x_1 + a_{i,2} x_2 + \ldots + a_{i,7} x_7 + b_i u$$

or in matrix notation

$$\dot{\mathbf{x}} = \mathbf{A}\, x + \mathbf{B}\, u$$

where $\dot{\mathbf{x}}$ is the vector of x_i, $\mathbf{B}$ is the vector of b_i, and u is the scalar input (independent variable). By transforming from the time domain into the Laplace domain the preceding equation in terms of the Laplace operator, s, for zero initial conditions becomes

$$s\, X\,(s) = \mathbf{A}\, X\,(s) + \dot{\mathbf{B}}\, u\,(s)$$

By rearrangement we have

$$[s\, I - \mathbf{A}] X\,(s) = \mathbf{B}\, u\,(s)$$

where I is the identity matrix. Therefore

$$X\,(s) = \text{adjoint}\,[(s\, I - \mathbf{A})/\det\,(s\, I - \mathbf{A})] \cdot \mathbf{B}\, u\,(s)$$

We are only concerned at this point with the transient response rather than the total (transient plus steady-state) response. The time response characteristics of the natural modes of the system are obtained from the characteristic equation obtained by setting the denominator of X (s) equal to zero.

$$\det\,(s\, I - \mathbf{A}) = 0$$

The determinant (det) is obtained by standard techniques (19) in algebraic form. This seventh-order polynomial expression is written in the form

$$O = C_0 s + C_1 s^1 + C_2 s^2 + \ldots + C_7 s^7$$

Because some of these coefficients C_n contain over 50 terms, they are not presented here, but they are available on request.[1] With these coefficients it is possible to obtain the roots of this expression used to predict the dynamic behavior of the system. The roots of the characteristic equation are the so-called eigenvalues of the matrix A.

[1] Coefficients C_n available on request from B. J. B. Grant, Pulmonary Div., University Hospital, Box 055, 1405 E. Ann St., Ann Arbor, MI 48109.

This work was supported by the Dorothy Temple Cross Travelling Fellowship (Medical Research Council, UK), the Parker B. Francis Foundation, the John F. Perkins, Jr. Memorial Fund, National Heart, Lung, and Blood Institute Grant HL-17331, the California Lung Association, and the University of Michigan Medical School Computing Fund.

Received 29 March 1982; accepted in final form 26 August 1982.

REFERENCES

1. BARER, G. R., P. HOWARD, AND J. W. SHAW. Stimulus-response curves for the pulmonary vascular bed to hypoxia and hypercapnia. *J. Physiol. London* 211: 139–155, 1970.
2. BARER, G. R., AND J. W. SHAW. Pulmonary vasodilator and vasoconstrictor actions of carbon dioxide. *J. Physiol. London* 213: 633–645, 1971.
3. BENUMOF, J. L., J. M. MATHERS, AND E. A. WAHRENBROCK. Cyclic hypoxic pulmonary vasoconstriction induced by concomitant carbon dioxide changes. *J. Appl. Physiol.* 41: 466–469, 1976.
4. BENUMOF, J. L., AND E. A. WAHRENBROCK. Blunted hypoxic pulmonary vasoconstriction by increased vascular pressures. *J. Appl. Physiol.* 38: 846–850, 1975.
5. BERGOFSKY, E. H., F. HAAS, AND R. PORCELLI. Determination of the sensitive vascular sites from which hypoxia and hypercapnia elicit rises in pulmonary arterial pressure. *Federation Proc.* 27: 1420–1425, 1968.
6. GOMEZ, D. M. Considerations of the oxygen-hemoglobin equilibrium in the physiological state. *Am. J. Physiol.* 200: 135–142, 1961.
7. GRANT, B. J. B. Effects of hypoxic pulmonary vasoconstriction on arterial oxygen tension. Distribution of pulmonary gas exchange. *INSERM* 51: 193–200, 1975.
8. GRANT, B. J. B. Regulation of local and overall pulmonary blood flow in a computer model of the lung (Abstract). *Clin. Sci.* 258: 110P, 1976.
9. GRANT, B. J. B. *The Effect of Local Alveolar Gas Tensions on Blood Flow to Small Lung Units* (MD thesis). London: Univ. of London, 1977.
10. GRANT, B. J. B. Effect of local pulmonary blood flow control on gas exchange: theory. *J. Appl. Physiol.: Respirat. Environ. Exercise Physiol.* 53: 1100–1109, 1982.
11. GRANT, B. J. B., E. E. DAVIS, H. JONES, AND J. M. B. HUGHES. Local regulation of pulmonary blood flow and ventilation-perfusion ratios in the coatimundi. *J. Appl. Physiol.* 40: 216–228, 1976.
12. HIGGINS, J. The theory of oscillating systems. *Ind. Eng. Chem.* 59: 19–62, 1967.
13. KELMAN, G. R. Digital computer subroutine for the conversion of oxygen tension into saturation. *J. Appl. Physiol.* 21: 1375–1376, 1966.
14. KELMAN, G. R. Calculation of certain indices of cardiopulmonary function using a digital computer. *Respir. Physiol.* 1: 335–343, 1966.
15. KELMAN, G. R. Digital computer procedure for conversion of P_{CO_2} into blood CO_2 content. *Respir. Physiol.* 3: 111–115, 1967.
16. MALIK, A. B., AND B. S. L. KIDD. Independent effects of changes in H^+ and CO_2 concentration on hypoxic pulmonary vasoconstriction. *J. Appl. Physiol.* 34: 318–323, 1973.
17. MALIK, A. B., AND B. S. L. KIDD. Time course of pulmonary vascular response to hypoxia in dogs. *Am. J. Physiol.* 224: 1–6, 1973.
18. PEAKE, M. D., A. L. HARABIN, N. J. BRENNAN, AND J. T. SYLVESTER. Steady-state vascular responses to graded hypoxia in isolated lungs of five species. *J. Appl. Physiol.* 51: 1214–1219, 1981.
19. RIGGS, D. S. *Control Theory and Physiological Feedback Mechanisms.* Baltimore, MD: Williams & Wilkins, 1970.
20. SIEGEL, B., H. ROEDEL, AND H. W. HOFER. Basic rhythms in vascular smooth muscle. Smooth muscle pharmacology and physiology. *INSERM* 50: 215–232, 1975.
21. SYLVESTER, J. T., A. L. HARABIN, M. D. PEAKE, AND R. S. FRANK. Vasodilator and constrictor responses to hypoxia in isolated pig lungs. *J. Appl. Physiol.: Respirat. Environ. Exercise Physiol.* 49: 820–825, 1980.
22. TUCKER, A., AND J. T. REEVES. Nonsustained pulmonary vasoconstriction during acute hypoxia in anesthetized dogs. *Am. J. Physiol.* 228: 756–761, 1975.
23. TUCKER, A., E. K. WEIR, J. T. REEVES, AND R. F. GROVER. Histamine H_1 and H_2 receptors in pulmonary and systemic vasculature of the dog. *Am. J. Physiol.* 229: 1108–1113, 1975.
24. TUCKER, A., E. K. WEIR, J. T. REEVES, AND R. F. GROVER. Failure of histamine antagonists to prevent hypoxic pulmonary vasoconstriction in dogs. *J. Appl. Physiol.* 40: 496–500, 1976.
25. VILES, P. H., AND J. T. SHEPHERD. Evidence for a dilator action of carbon dioxide on pulmonary vessels of the cat. *Circ. Res.* 22: 325–332, 1968.
26. VILES, P. H., AND J. T. SHEPHERD. Relationship between pH, pO_2, and pCO_2 on the pulmonary vascular bed of the cat. *Am. J. Physiol.* 215: 1170–1176, 1968.
27. WEST, J. B., AND P. D. WAGNER. Pulmonary gas exchange. In: *Bioengineering Aspects of the Lung.* New York: Dekker, 1977, vol. 3, p. 361–457. (Lung Biol. Health Dis. Ser.)